Electronic Supplementary Material (ESI) for Nanoscale.
This journal is © The Royal Society of Chemistry 2023

Supporting Information

Transparent Metal Oxide Interlayer Enabling Durable and Fast-switching Zinc Anode-Based Electrochromic Devices

Bing Xu,[a] Jingwei Chen,*[a] Ping Li,[a] Yujia Ouyang,[a] Yu Ma,[a] Huanlei Wang,*[a] Haizeng Li *[b]

[a] School of Materials Science and Engineering, Ocean University of China, Qingdao 266100, China. E-mail: chenjingwei@ouc.edu.cn; huanleiwang@ouc.edu.cn

[b] Institute of Frontier & Interdisciplinary Science, Shandong University, Qingdao 266237, China. E-mail: haizeng@sdu.edu.cn

1. Morphology and compositional characterization.

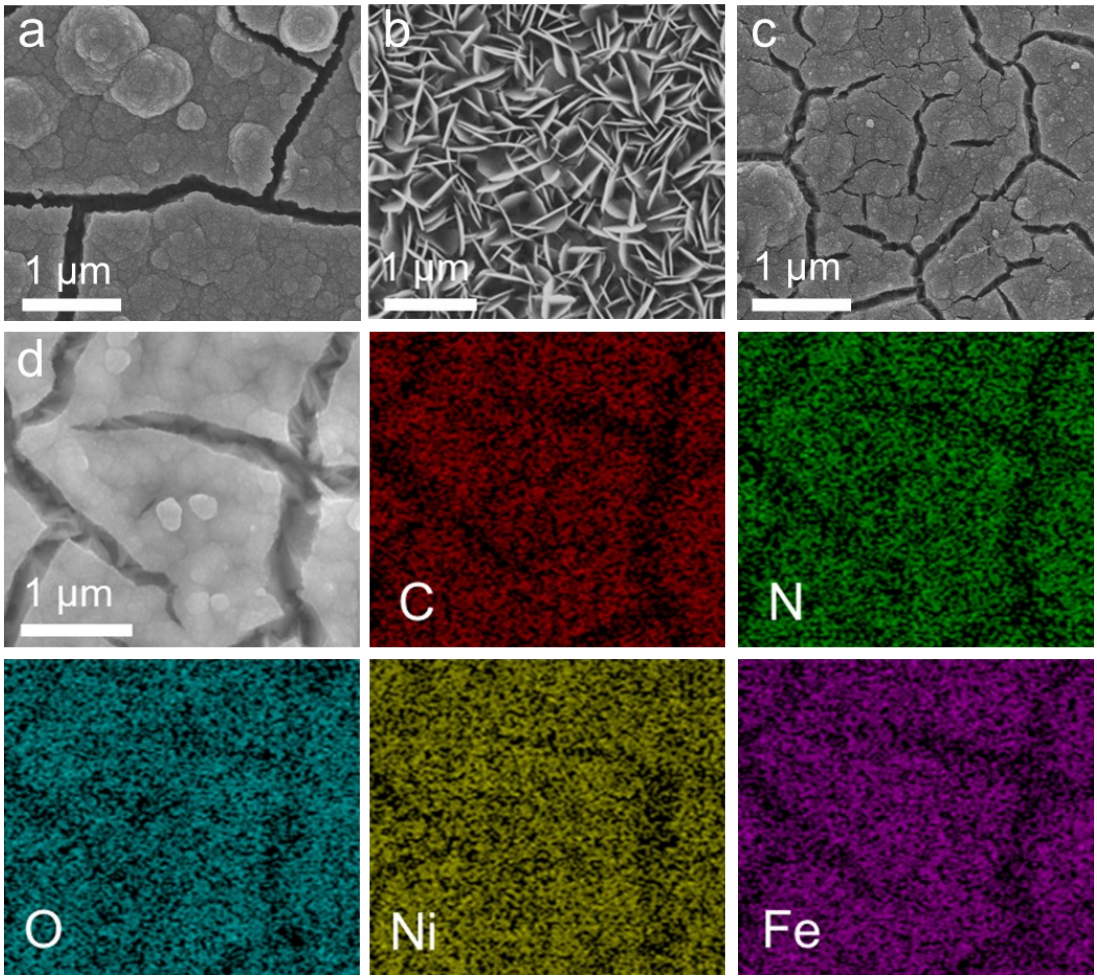

Figure S1. SEM images of a) PB, b) $Ni(OH)_2$, c) $Ni(OH)_2$/PB. d) SEM image and corresponding elemental mapping of NiO/PB.

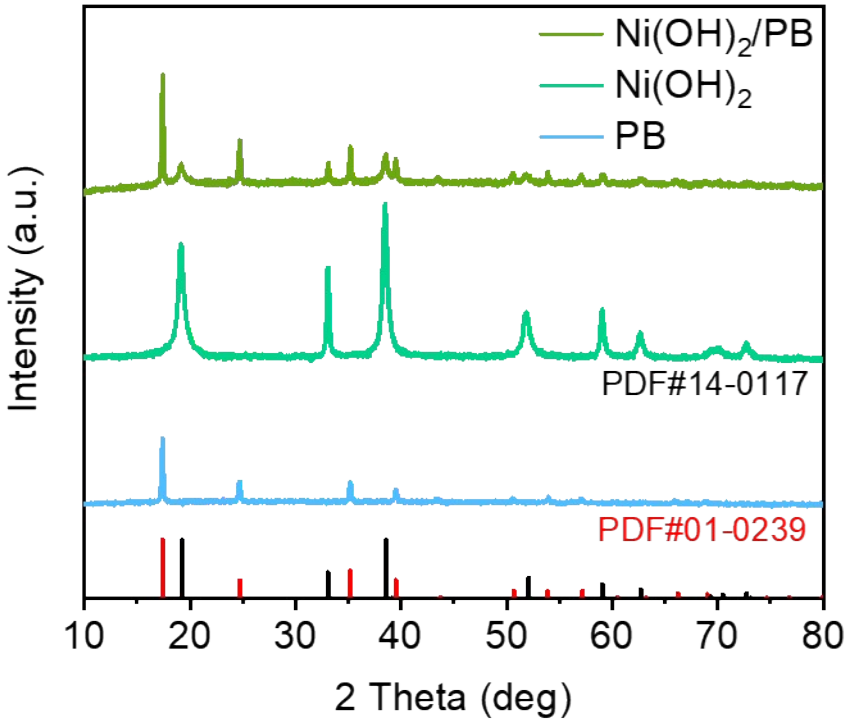

Figure S2. XRD plots of PB, $Ni(OH)_2$ and $Ni(OH)_2$/PB.

2. Electrochemical performance characterization.

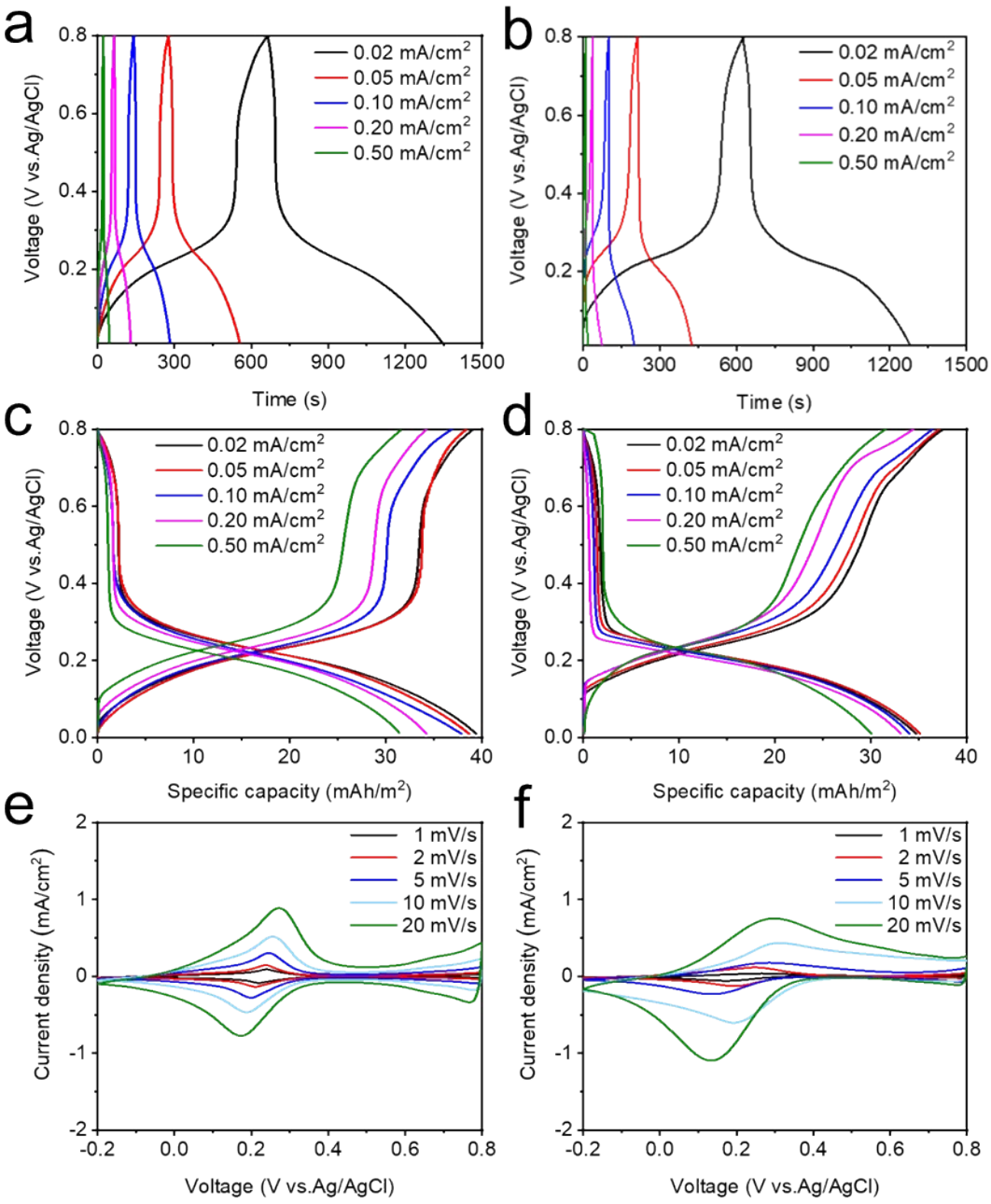

Figure S3. Electrochemical performance of PB and $Ni(OH)_2$/PB. GCD curves of a) PB and b) $Ni(OH)_2$/PB at different current densities. Areal specific capacity curves of c) PB and d) $Ni(OH)_2$/PB at different current densities. CV curves of e) PB and f) $Ni(OH)_2$/PB under various sweep rates.

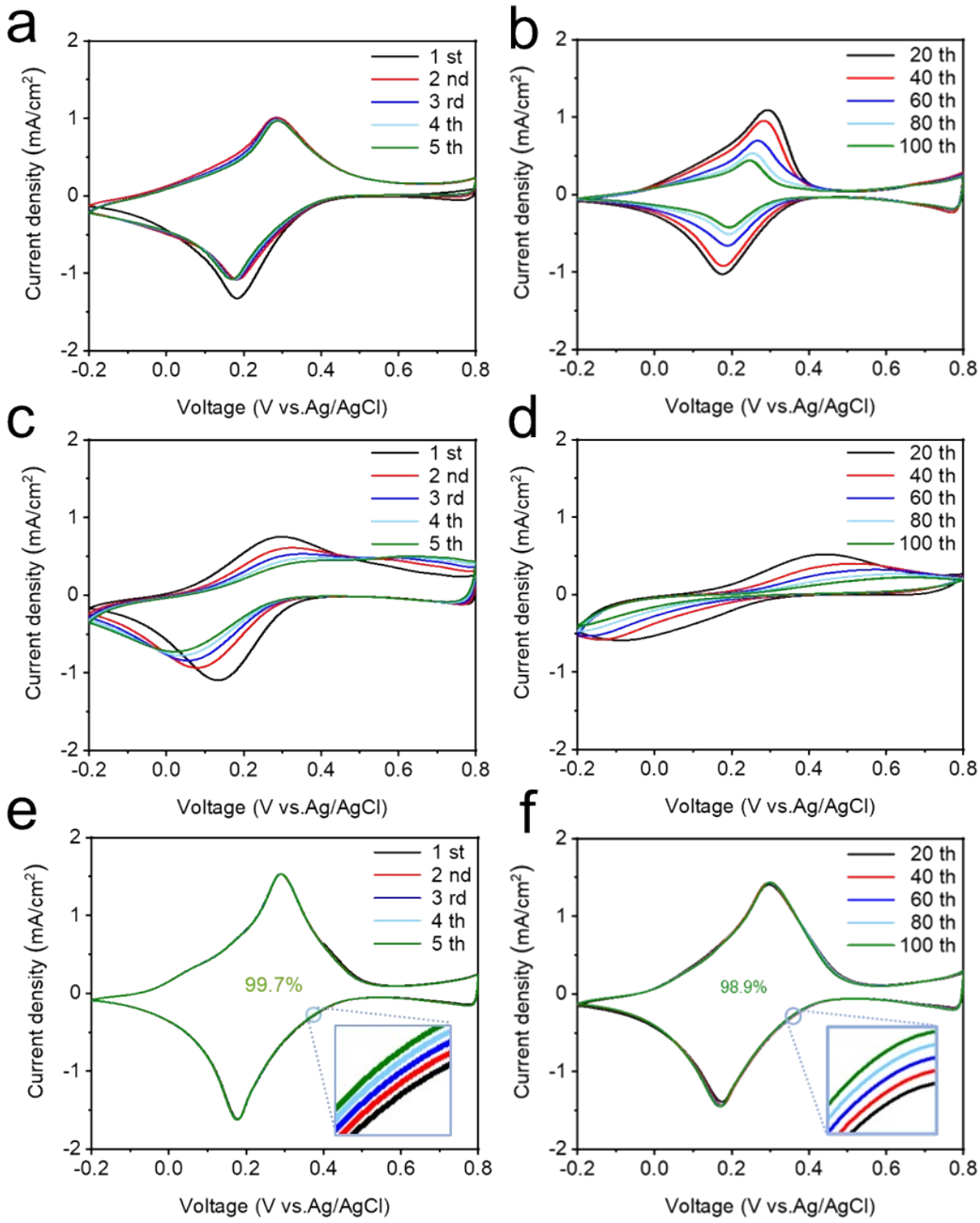

Figure S4. CV curves for the first 5 cycles of a) PB, c) $Ni(OH)_2$/PB and e) NiO/PB at scan rate of 20 mV/s. CV curves for the first 100 cycles of b) PB, d) $Ni(OH)_2$/PB, and f) NiO/PB at a scan rate of 20 mV/s.

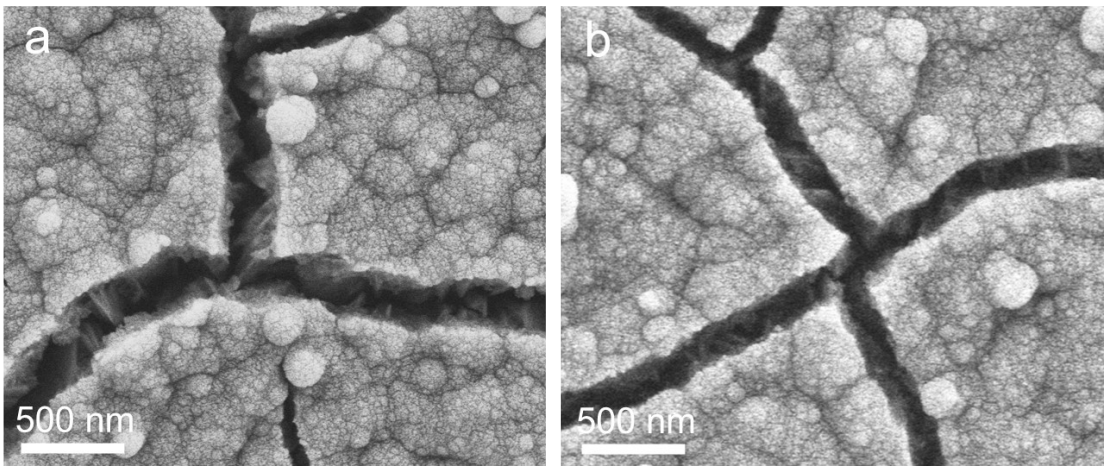

Figure S5. SEM images of NiO/PB a) before and b) after cycling (CV).

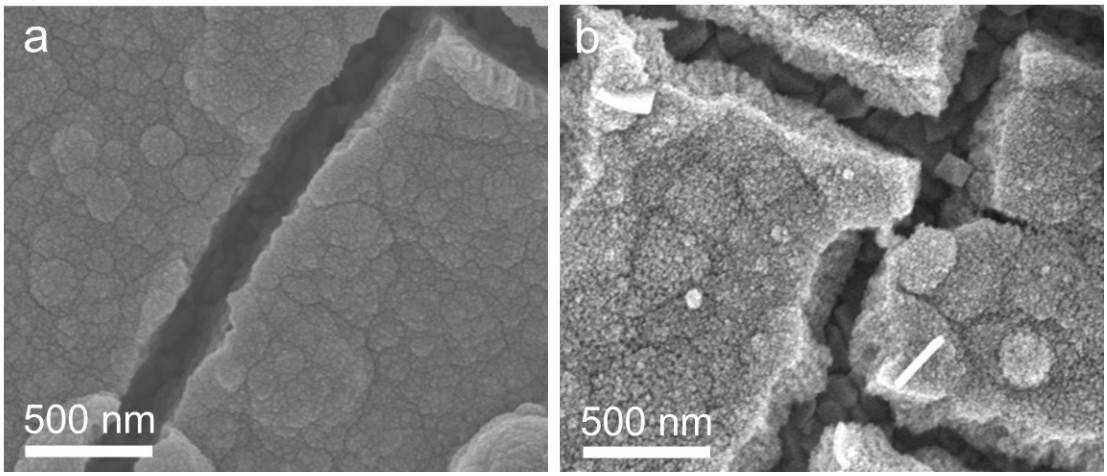

Figure S6. SEM images of PB a) before and b) after cycling (CV).

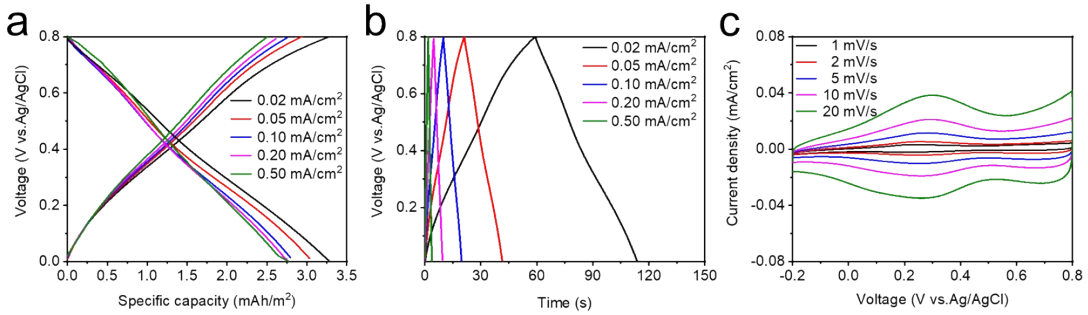

Figure S7. a, b) GCD curves of NiO at different current densities. c) CV curves of NiO under various sweep speeds.

3. Electrochromic performance characterization.

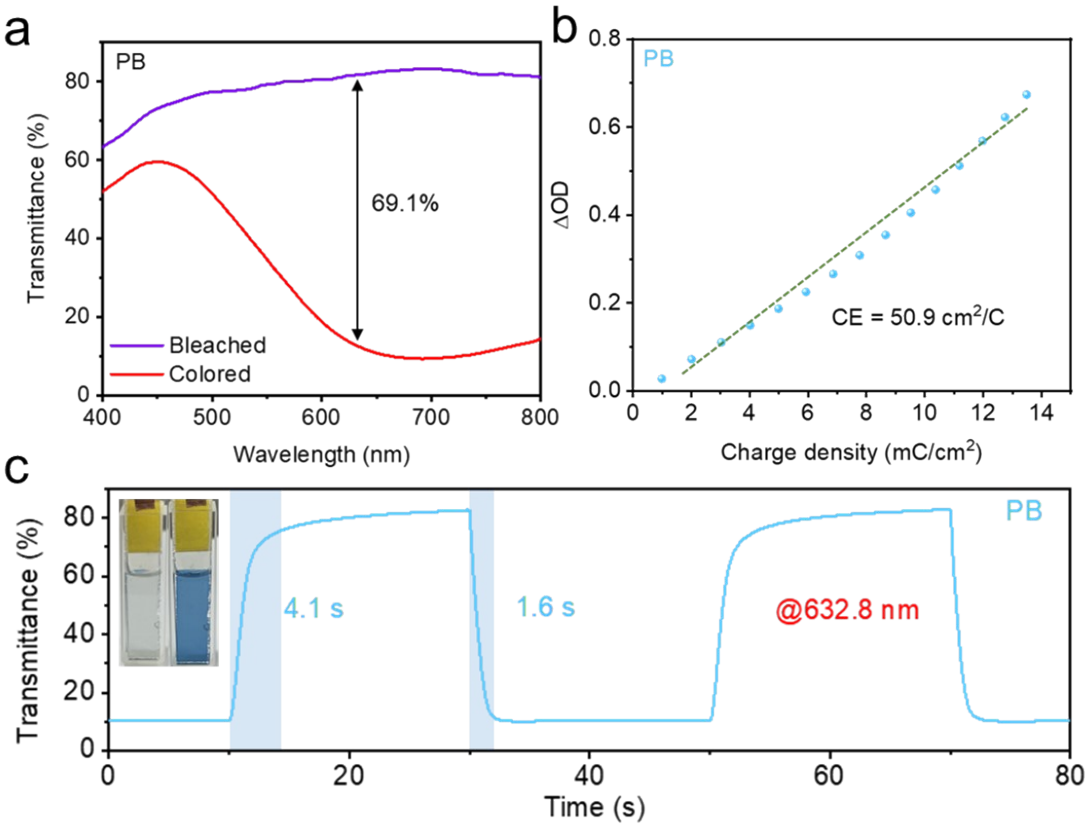

Figure S8. Electrochromic performance of PB. a) Transmittance spectra of PB in colored and bleached states at 400-800 nm. b) In-situ optical density versus charge density at 632.8 nm for PB during coloration. c) In-situ transmittance response of PB at 632.8 nm under potential steps (0.6 V and 1.8 V, each for 20 s), and digital photographs of PB in both colored and bleached states (inset).

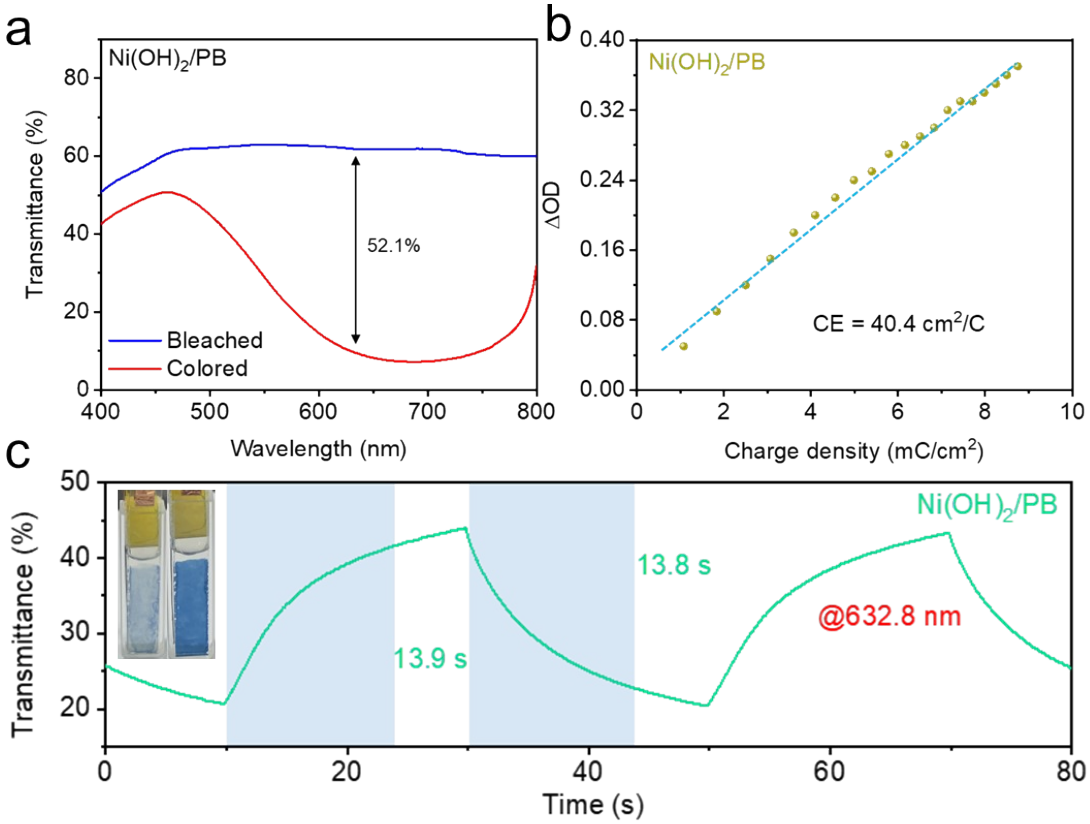

Figure S9. Electrochromic performance of $Ni(OH)_2$/PB. a) Transmittance spectra of $Ni(OH)_2$/PB in colored and bleached states at 400-800 nm. b) In-situ optical density versus charge density at 632.8 nm for $Ni(OH)_2$/PB during coloration. c) In-situ transmittance response of $Ni(OH)_2$/PB at 632.8 nm under potential steps (0.6 V and 1.8 V, each for 20 s), and digital photographs of $Ni(OH)_2$/PB in both colored and bleached states (inset).

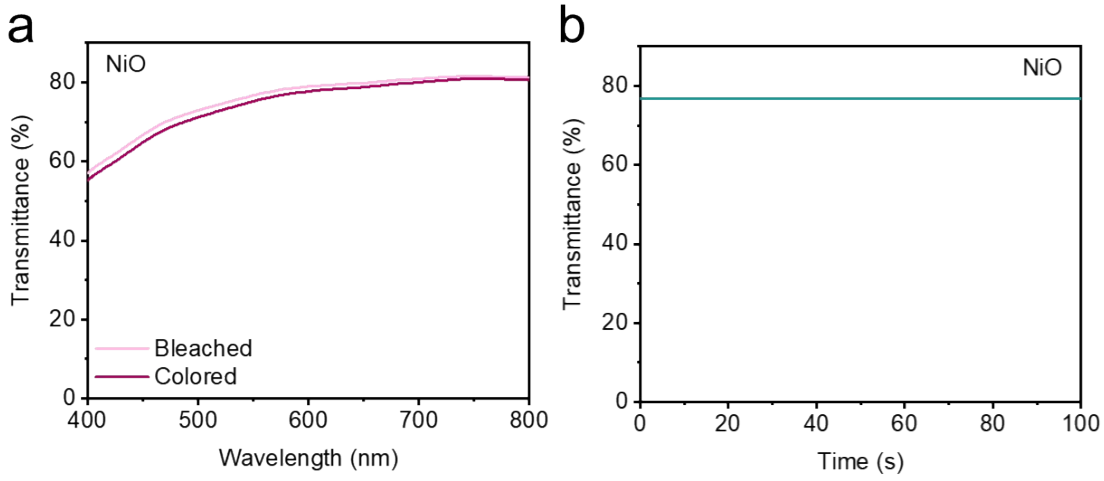

Figure S10. a) Transmittance spectra of NiO/PB in colored and bleached states at 400-800 nm. b) In-situ transmittance response of NiO at 632.8 nm under potential steps (0.6

V and 1.8 V, each for 20 s).

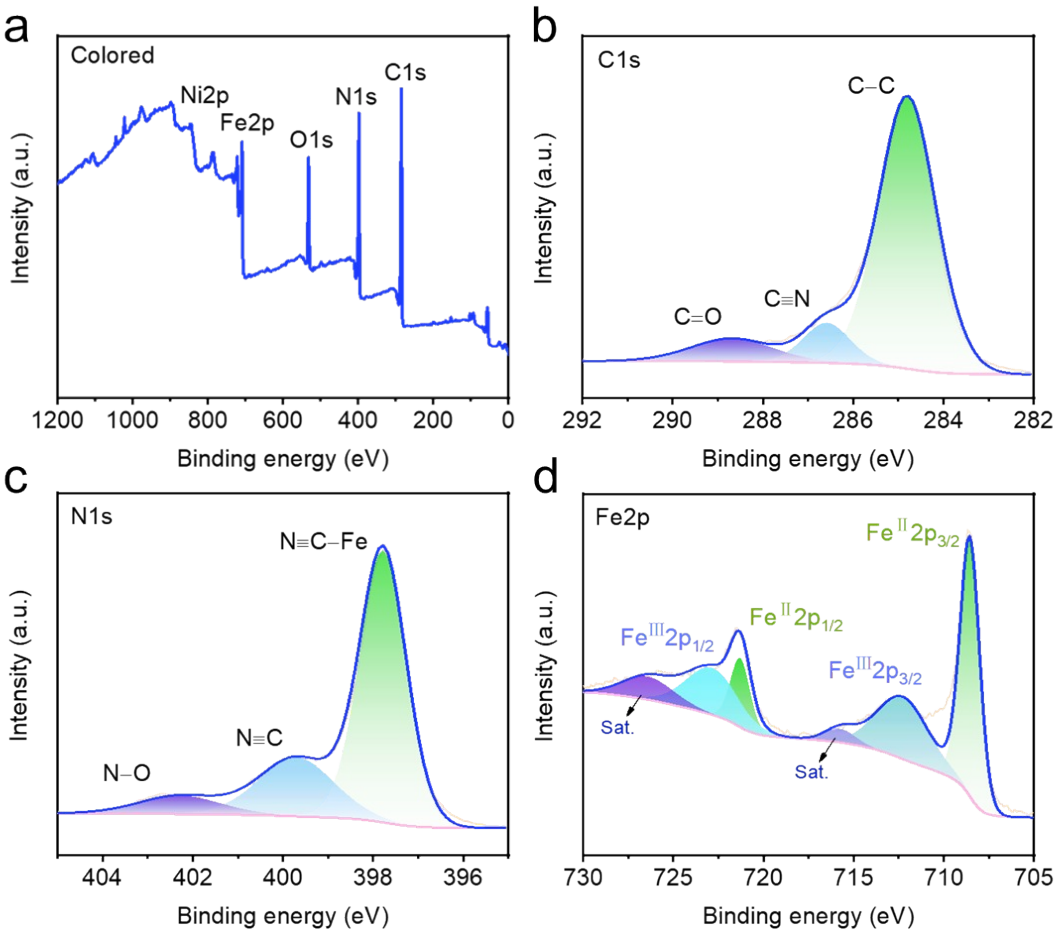

Figure S11. a) XPS survey spectrum of NiO/PB in colored state. High resolution XPS spectra of b) C1s, c) N1s, and d) Fe2p.

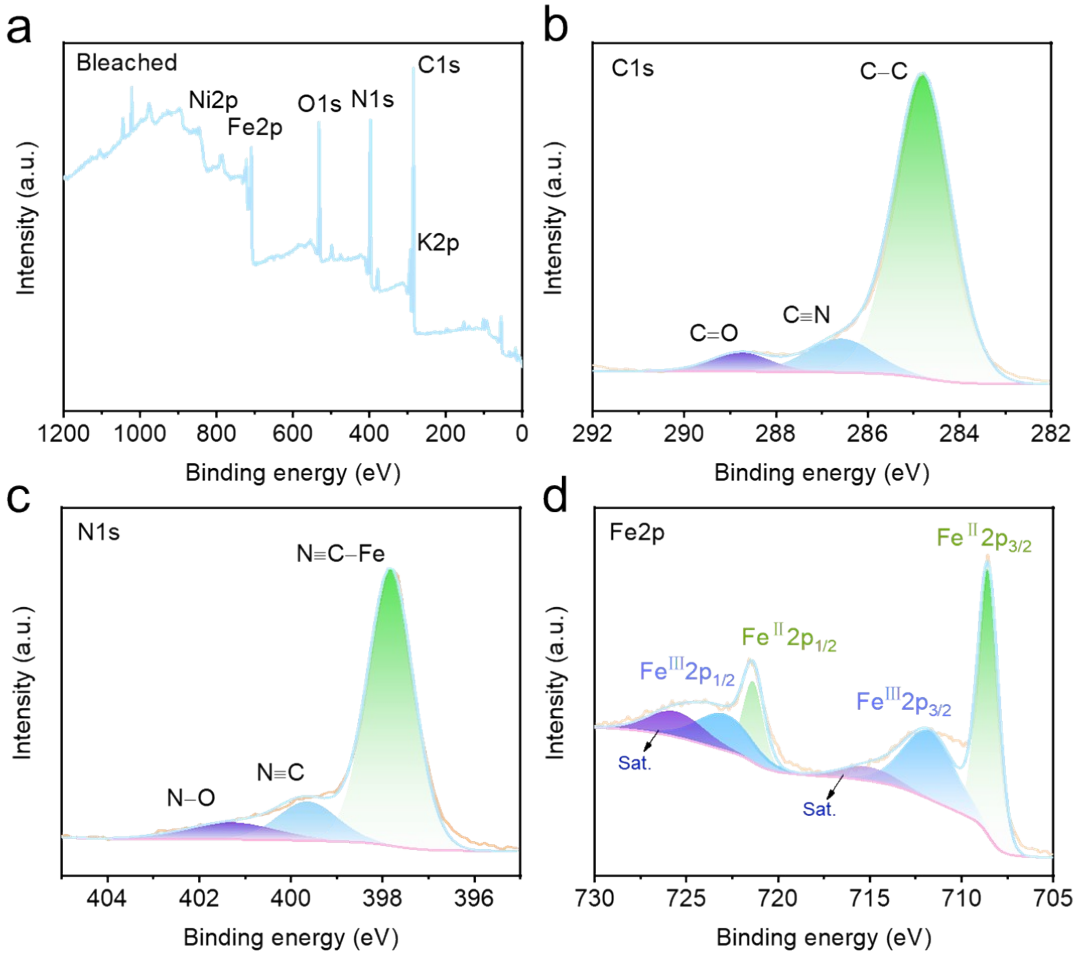

Figure S12. a) XPS survey spectrum of NiO/PB in bleached state. High resolution XPS spectra of b) C1s, c) N1s, and d) Fe2p.

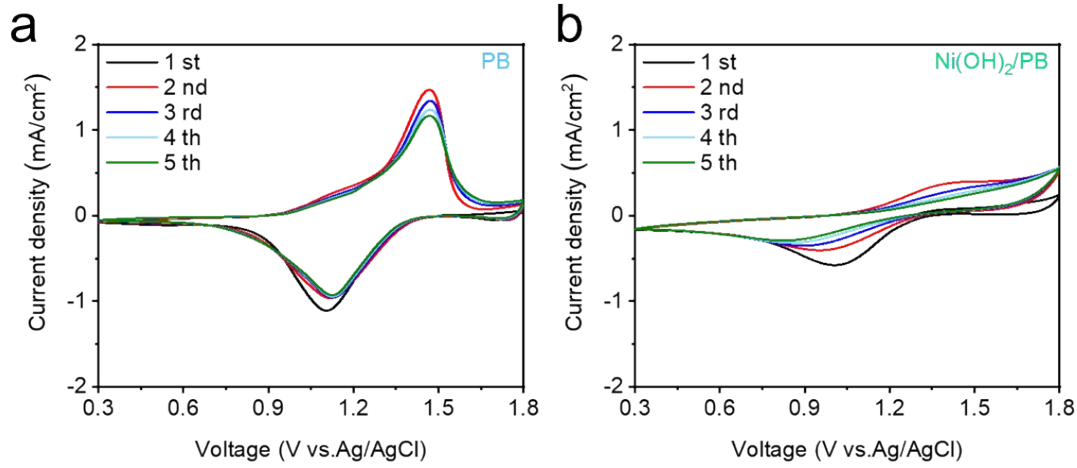

Figure S13. CV curves of zinc-anode based electrochromic devices with a) PB and b) $Ni(OH)_2$/PB cathodes for the first 5 cycles at 20 mV/s.

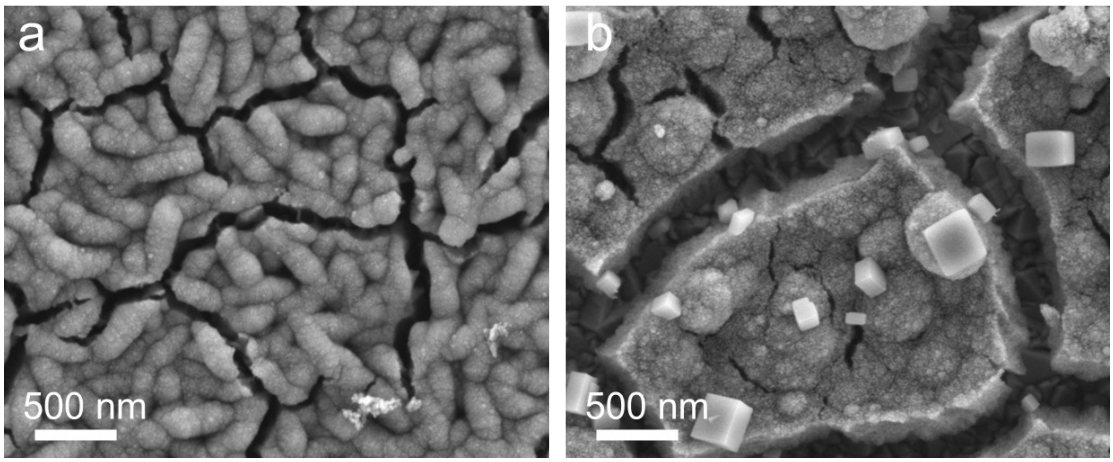

Figure S14. SEM images of a) NiO/PB and b) PB after 1000 cycles.

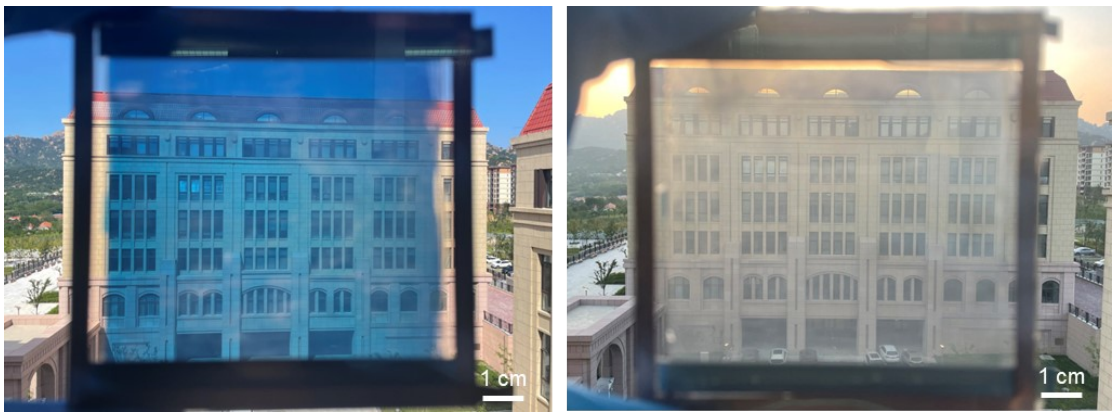

Figure S15. Digital photographs of 10 cm*10 cm zinc-anode based electrochromic device in colored (left) and bleached (right) state.

Table S1. Comparison of electrochromic performance of some research on PB.

	❒T	**t_c (s)**	**t_b (s)**	**CE (cm^2 C^{-1})**	**Durability**
Au/PB[1]	66% (700 nm)	1.4	2.2	131	96% (2000 cycles)
TASA/PB[2]	50% (700 nm)	6.6	3.2	93	85% (1000 cycles)
PB[3]	68% (700 nm)	4.7	7.5	117	78% (1000 cycles)
TiO_2@PB[4]	48% (700 nm)	6.2	2.2	131	-
TNRA@G/PB[5]	56% (700 nm)	1	2.8	129	97% (1000 cycles)
wPB[6]	63% (545 nm)	10	10	157	93% (1000 cycles)
PB[7]	60% (633 nm)	8	12	116	77% (1200 cycles)
PB/P5ICA[8]	39% (680 nm)	2.2	7.8	262	83% (1000 cycles)
This work	73% (633 nm)	1.4	2.6	55	92% (1000 cycles)

References

1. M. Xu, S. Wang, S. Zhou, Z. Ding, H. Xu, J. Zhao and Y. Li, *Advanced Materials Interfaces,* 2023, **10**, 2201765.
2. Y. Wang, X. Jia, M. Zhu, X. Liu and D. Chao, *New Journal of Chemistry*, 2020, **44**, 8138-8147.
3. Y. Ding, H. Sun, Z. Li, C. Jia, X. Ding, C. Li, J.-G. Wang and Z. Li, *Journal of Materials Chemistry A*, 2023, **11**, 2868-2875.
4. Y. Chen, Z. Bi, X. Li, X. Xu, S. Zhang and X. Hu, *Electrochimica Acta*, 2017, **224**, 534-540.
5. Y. Wang, Z. Gong, Y. Zeng, H. Zhao and J. Yang, *Chemical Engineering Journal*, 2022, **431**, 134066.
6. M.-S. Fan, S.-Y. Kao, T.-H. Chang, R. Vittal and K.-C. Ho, *Solar Energy Materials and Solar Cells*, 2016, **145**, 35-41.
7. J. Song, B. Huang, S. Liu, L. Kang, Z. Zhang, G. Shang, Y. Yang, X. Li and D. Wang, *Solar Energy*, 2022, **232**, 275-282.
8. Q. Li, B. Wang, H. Zou, Q. Guo and G. Nie, *Journal of Alloys and Compounds*, 2022, **921**, 166140.